

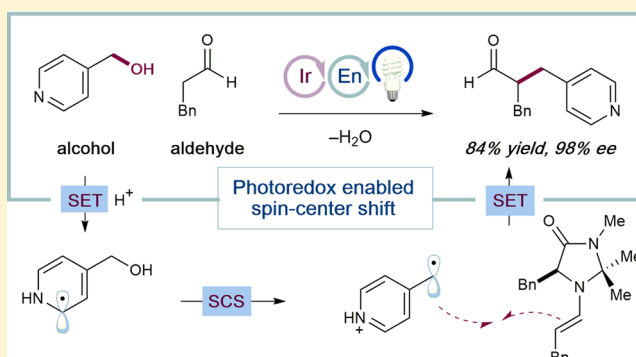
Spin-Center Shift-Enabled Direct Enantioselective α -Benzylation of Aldehydes with Alcohols

Eric D. Nacsa and David W. C. MacMillan*¹

Merck Center for Catalysis, Princeton University, Washington Road, Princeton, New Jersey 08544, United States

S Supporting Information

ABSTRACT: Nature routinely engages alcohols as leaving groups, as DNA biosynthesis relies on the removal of water from ribonucleoside diphosphates by a radical-mediated “spin-center shift” (SCS) mechanism. Alcohols, however, remain underused as alkylating agents in synthetic chemistry due to their low reactivity in two-electron pathways. We report herein an enantioselective α -benzylation of aldehydes using alcohols as alkylating agents based on the mechanistic principle of spin-center shift. This strategy harnesses the dual activation modes of photoredox and organocatalysis, engaging the alcohol by SCS and capturing the resulting benzylic radical with a catalytically generated enamine. Mechanistic studies provide evidence for SCS as a key elementary step, identify the origins of competing reactions, and enable improvements in chemoselectivity by rational photocatalyst design.



INTRODUCTION

In DNA biosynthesis, deoxyribonucleoside diphosphate building blocks are procured from their corresponding ribonucleosides by the action of ribonucleotide reductase (RNR) enzymes.¹ The key step in this deoxygenation occurs via a (3',2')-spin-center shift (SCS) event, which induces a β -C–O scission and the net loss of water (Figure 1a).² Despite this well-established open-shell mechanism that engages alcohols as leaving groups, alcohols remain underexploited as alkylating agents due to the substantial barrier to the displacement of the hydroxyl group by two-electron pathways.³ Nonetheless, the direct use of alcohols as electrophiles remains an important goal in synthetic organic chemistry due to their low genotoxicity, robustness, and ubiquity in naturally occurring molecules.⁴

Inspired by nature's spin-center shift process, our group recently reported the alkylation of heteroarenes with alcohols as latent alkylating agents, relying on dual photoredox and hydrogen atom transfer catalysis.⁵ Given that photoredox catalysis provides (1) mild access to open-shell radical intermediates and (2) a general platform to perform concurrent oxidation and reduction steps in the same vessel,⁶ we hypothesized that this activation mode, in concert with organocatalysis, could enable a direct, enantioselective α -benzylation of aldehydes with heterobenzylic alcohols as electrophiles by exploiting SCS (Figure 1b).

Pioneering work by Evans et al.,⁷ Oppolzer et al.,⁸ Seebach et al.,⁹ and Myers et al.¹⁰ has long established that the stereoselective α -benzylation of carbonyls can be readily accomplished using chiral auxiliaries. Surprisingly, however, catalytic enantioselective variants of this important transformation have been slower to develop, with the most notable

examples being the phase transfer benzylation of glycine imines,¹¹ chiral triamine ligation of ketone-derived lithium enolates,¹² and Cr(salen) activation of preformed tin enolates.¹³ More recently, photoredox organocatalysis has emerged as a platform for the enantioselective construction of α -alkylated carbonyl motifs,¹⁴ including the α -benzylation of aldehydes using electron-deficient benzylic bromides.^{14b}

A common feature of both catalytic and auxiliary-based strategies is the reliance on benzylic halide electrophiles or their equivalents (e.g., tosylates). Indeed, alkyl (pseudo)halides are archetypal alkylating agents due to the excellent leaving group ability of bromide, iodide, and sulfonate ions. This reactivity, however, also confers undesirable properties, such as genotoxicity and light-sensitivity, necessitating care in handling and storing these reagents. Furthermore, alkyl halides are frequently obtained by treatment of the corresponding alcohols with a stoichiometric activating agent,¹⁵ highlighting the appeal of engaging alcohols directly. In the context of asymmetric α -alkylation, the use of alcohols has been restricted to specialized cases where heterolytic C–O cleavage generates highly stabilized cations.¹⁶ In this paper, we report the design and application of an enantioselective α -benzylation of aldehydes with heterobenzylic alcohols as well as mechanistic studies that support the proposed SCS pathway, elucidate the major undesired reaction pathways, and enable improvements in chemoselectivity by photocatalyst modification.

Received: December 2, 2017

Published: February 5, 2018

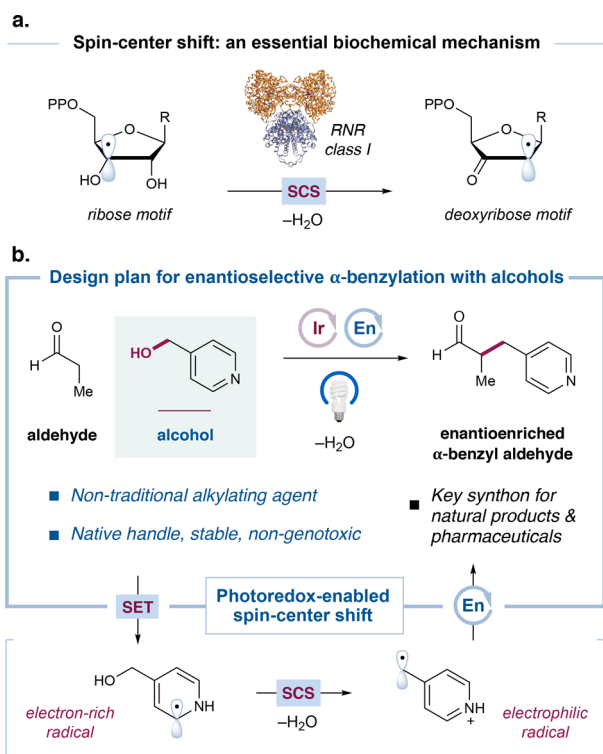


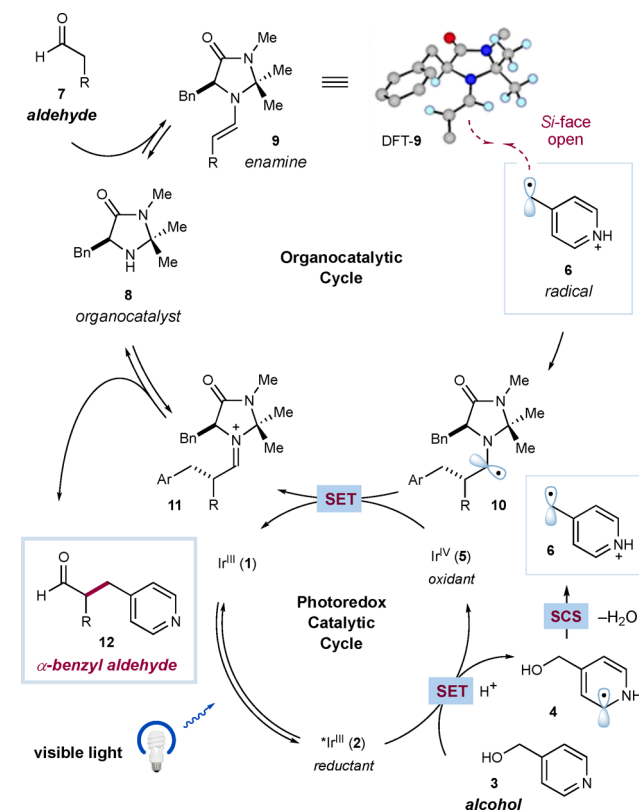
Figure 1. Spin-center shift (SCS) as a conceptual basis for the enantioselective α -benzylation of aldehydes with alcohols. (a) SCS in DNA biosynthesis. (b) Advantages of alcohols as alkylating agents and a possible mechanism in which benzylic alcohols may be engaged by SCS.

DESIGN PLAN

Our design for the enantioselective α -benzylation of aldehydes with alcohols is outlined in **Figure 1b**. Single-electron reduction of a benzylic alcohol by a photoredox catalyst would initially give rise to an electron-rich radical. This intermediate would be poised to undergo SCS, whereby benzylic C–O bond cleavage and proton transfer would expel a molecule of water and reveal an electrophilic benzylic radical. This electron-deficient species would then react with a catalytically generated enamine, forming the desired C–C bond stereoselectively and ultimately leading to the enantioenriched α -benzyl aldehyde.

A detailed mechanistic description of the proposed transformation is shown in **Scheme 1**. Excitation of an Ir^{III} catalyst (**1**) with blue light would first generate a long-lived ^{*}Ir^{III} excited state (**2**) [$\tau = 1.90 \mu\text{s}$ for Ir(ppy)₃].¹⁷ This highly reducing species $\{E_{1/2}^{\text{red}}[\text{Ir}^{\text{IV}}/\text{*Ir}^{\text{III}}] = -1.81 \text{ V}$ vs saturated calomel electrode (SCE) in CH₃CN for Ir(ppy)₃\} should reduce a protonated heterobenzylic alcohol such as 4-(hydroxymethyl)pyridine (**3**, $E^{\text{red}} = -1.29 \text{ V}$ vs SCE in CH₃CN for 3-HBr) to furnish electron-rich radical **4** and Ir^{IV} intermediate **5**. Radical **4** would then undergo the key spin-center shift event to unveil electrophilic radical **6** and extrude a molecule of water after proton transfer. Within the same time frame, aldehyde **7** and an organocatalyst (**8**) would condense to form chiral enamine **9**. The depicted DFT structure of **9** (with propionaldehyde as the aldehyde) illustrates that the benzyl substituent of the organocatalyst shields the *Re*-face of the enamine, leaving the *Si*-face exposed for reaction with electrophilic radical **6**. The resulting α -amino radical **10** ($E_{1/2}^{\text{ox}} = -1.12$ to -0.92 V vs SCE in CH₃CN for simple α -

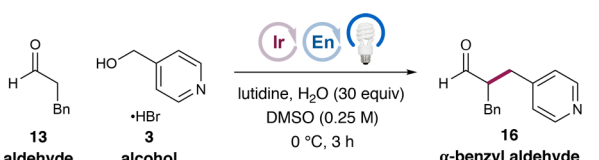
Scheme 1. Proposed Mechanism for the Enantioselective α -Benzylation of Aldehydes with Alcohols



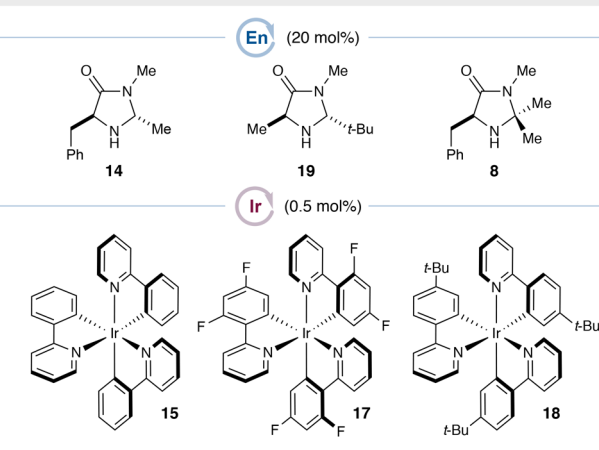
amino radicals)¹⁸ would be readily oxidized by the Ir^{IV} intermediate **5** $\{E_{1/2}^{\text{red}}[\text{Ir}^{\text{IV}}/\text{III}] = +0.77 \text{ V}$ vs SCE in CH₃CN for Ir(ppy)₃\} to regenerate ground-state Ir^{III} photocatalyst **1** and iminium ion **11**. Finally, hydrolysis of the latter species would liberate enantioenriched α -benzyl aldehyde **12** and organocatalyst **8**.

RESULTS

We first tested this hypothesis by subjecting hydrocinnamaldehyde (**13**) and alcohol **3**, as its trifluoroacetic acid salt, to the reaction conditions that proved optimal in the enantioselective α -benzylation of aldehydes using benzylic bromides^{14b} [20 mol % **14** as the organocatalyst, 0.5 mol % Ir(ppy)₃ (**15**) as the photocatalyst, and 3 equiv lutidine in DMSO at rt] under blue-light irradiation (**Table 1**, entry 1). While none of the desired product was obtained, omitting the lutidine base (entry 2) gave rise to the desired α -benzyl aldehyde **16** in promising yield (37%) and enantioselectivity (62% ee). We postulate that a more acidic medium is necessary to facilitate both the reduction of alcohol **3** via protonation and ultimately the required spin-center shift event. Optimization of the reaction conditions [see **Tables S1–S6**, Supporting Information (SI)] revealed that employing a substoichiometric amount of lutidine (25 mol %) and HBr as the acid, a 2-fold dilution of the mixture, the addition of water (30 equiv), and cooling the mixture to 0 °C provided **16** in 48% yield and much improved 90% ee (entry 3). The modest efficiency was due primarily to the net reduction of alcohol **3** to 4-methylpyridine, rather than low consumption of **3**, so we surmised that a less reducing photocatalyst such as fluorinated Ir^{III} complex **17**¹⁹ would minimize the production of the reduction byproduct. We were surprised, however, to observe a diminished 18% yield (entry

Table 1. Optimization of the Enantioselective α -Benzylation of Aldehydes with Alcohols^a


entry	lutidine	conditions	catalysts	yield	ee
1 ^b	300 mol%	no H ₂ O, 0.5 M, r.t.	14 + 15	0%	n.d.
2 ^b	0 mol%	no H ₂ O, 0.5 M, r.t.	14 + 15	37%	62%
3	25 mol%	as shown	14 + 15	48%	90%
4	25 mol%	as shown	14 + 17	18%	n.d.
5	25 mol%	as shown	14 + 18	78%	92%
6 ^c	50 mol%	DMA solvent	14 + 18	90%	92%
7 ^c	50 mol%	DMA solvent	19 + 18	6%	n.d.
8 ^c	50 mol%	DMA solvent, 6 h	8 + 18	88%	98%



^aAlcohol **3** (0.1 mmol), aldehyde **13** (1.5 equiv), lutidine, water, organocatalyst, and photocatalyst were irradiated in the indicated solvent with a 34 W blue LED lamp. Yields were determined by ¹H NMR. Enantioselectivities were determined by chiral HPLC analysis following reduction of the crude aldehyde to the corresponding alcohol. ^bTrifluoroacetic acid salt of the alcohol instead of the HBr salt. ^cAldehyde **13** (2.0 equiv).

4). Instead, the more reducing photocatalyst **18**¹⁷ improved efficiency without compromising enantioselectivity (entry 5, 78% yield, 92% ee; see later text for a detailed discussion). Further modification of stoichiometries and conducting the reaction in *N,N*-dimethylacetamide (DMA) gave optimal efficiency (90% yield, entry 6). Finally, while the sterically demanding *tert*-butyl organocatalyst **19** was unproductive (entry 7), catalyst **8**, featuring a fully substituted aminal, provided **16** in 88% yield and 98% ee after 6 h (entry 8). Further photocatalyst modifications could improve the chemoselectivity and thus the yield (see Figure 3), but **18** proved optimal when considering alcohol conversion and synthetic accessibility (see the SI).

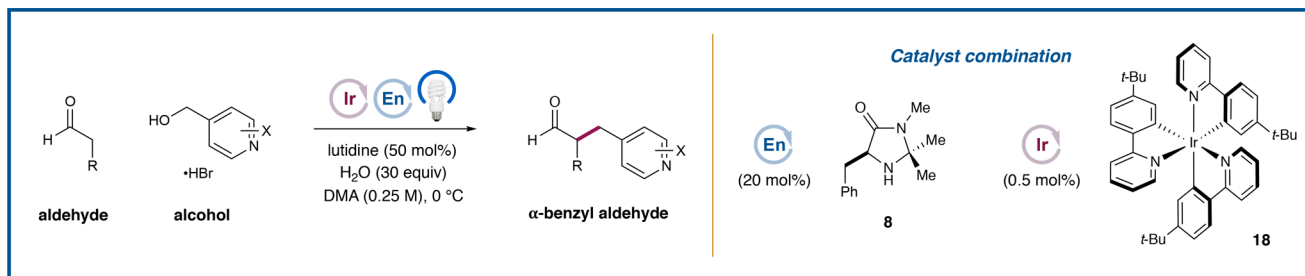
With this optimized set of conditions, we evaluated the scope of the enantioselective α -benzylation of aldehydes with alcohols (Table 2). First, a range of aldehydes undergo efficient and highly enantioselective benzylation with 4-(hydroxymethyl)pyridine (**3**). Hydrocinnamaldehyde was alkylated to give **16** in 84% isolated yield and 98% ee, consistent with smaller-scale optimization studies. A dimethoxy-substituted analogue (**20**) was also obtained in excellent efficiency and selectivity (86%

yield, 98% ee). β -Branched aldehydes are competent substrates, with cyclohexyl and piperidinyl products **21** and **22** obtained in good yields (86% and 80%, respectively) and enantioselectivities (96% and 94% ee, respectively). Simple alkanals such as octanal and propionaldehyde also reacted cleanly to give **23** (90% yield, 96% ee) and **24** (93% yield, 96% ee). Finally, unsaturation is tolerated, as shown by the production of alkene **25** (85% yield, 4.5:1 *Z/E*, 95% ee) and alkyne **26** (89% yield, 97% ee).

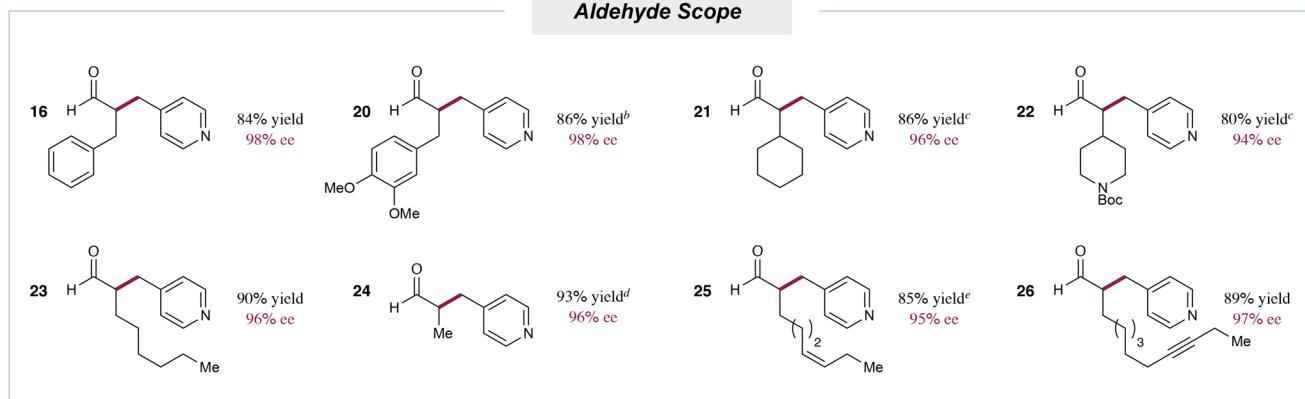
With respect to the heterobenzylic alcohol, a variety of substituted pyridines are competent in the reaction with hydrocinnamaldehyde. Methyl substitution at the 2-position or disubstitution at the 2- and 6-positions were well-tolerated, as were 2-phenyl or protected 2-amino substituents (**27–30**, 72–82% yield, 97–98% ee). The 3-position can also be substituted, with methyl-, methoxy-, fluoro-, and chloro-containing products **31–34** obtained in good yields (69–78%) and excellent enantioselectivities (94–98% ee). Quinolines are also capable of inducing the requisite spin-center shift, and a variety of substitution patterns about this aromatic motif are accommodated in the α -benzylation of hydrocinnamaldehyde. Specifically, 4-(hydroxymethyl)quinoline served as a competent alkylating agent, furnishing product **35** in 83% yield and 96% ee. The 2-methyl analogue (**36**) was also cleanly isolated (75% yield, 98% ee). Alcohols bearing substituents at the 6-position of the quinoline system can be employed and gave rise to products **37–39** containing fluoro, bromo, and protected oxygen functionalities in synthetically useful yields (60–70%) without compromising enantioselectivity (97–99% ee). Finally, 7-chloroquinoline **40** was also isolated in 76% yield and 99% ee.

Products obtained by this enantioselective α -benzylation possess enantioenriched homobenzylic stereocenters and a versatile aldehyde functional handle and, thus, may serve as important synthons for the preparation of bioactive molecules. To demonstrate the utility of this protocol, we sought to prepare the stereoselective ligand of translocator protein (18 kDa), PK-14067 (**44**, Figure 2).²⁰ To this end, propionaldehyde (**41**) was alkylated directly by alcohol **42**. The crude aldehyde (not shown) was oxidized to the corresponding carboxylic acid, and subsequent HATU-mediated coupling with diethylamine provided amide **43** in 79% yield and 95% ee over three steps. Finally, the phenyl substituent was installed in modest efficiency via a Minisci-type arylation²¹ to afford the target (**44**) in 52% yield and without erosion of enantiopurity. It is noteworthy that this synthesis corroborates the assigned (*R*)-configuration of the active isomer. Previous studies of PK-14067 had obtained this compound by racemic synthesis, followed by resolution, and assigned the configuration of the bioactive enantiomer by comparison of its experimental VCD spectrum to the simulated spectrum of both enantiomers.²² The known stereochemical course of our α -benzylation (see the SI for a discussion) reliably delivered (*R*)-**44**, the optical rotation of which (95% ee, $[\alpha]_D = -88^\circ$, $c = 1.0$, EtOH) matched the reported value for the active enantiomer (99% ee, $[\alpha]_D = -90^\circ$, $c = 2.86$, EtOH).²²

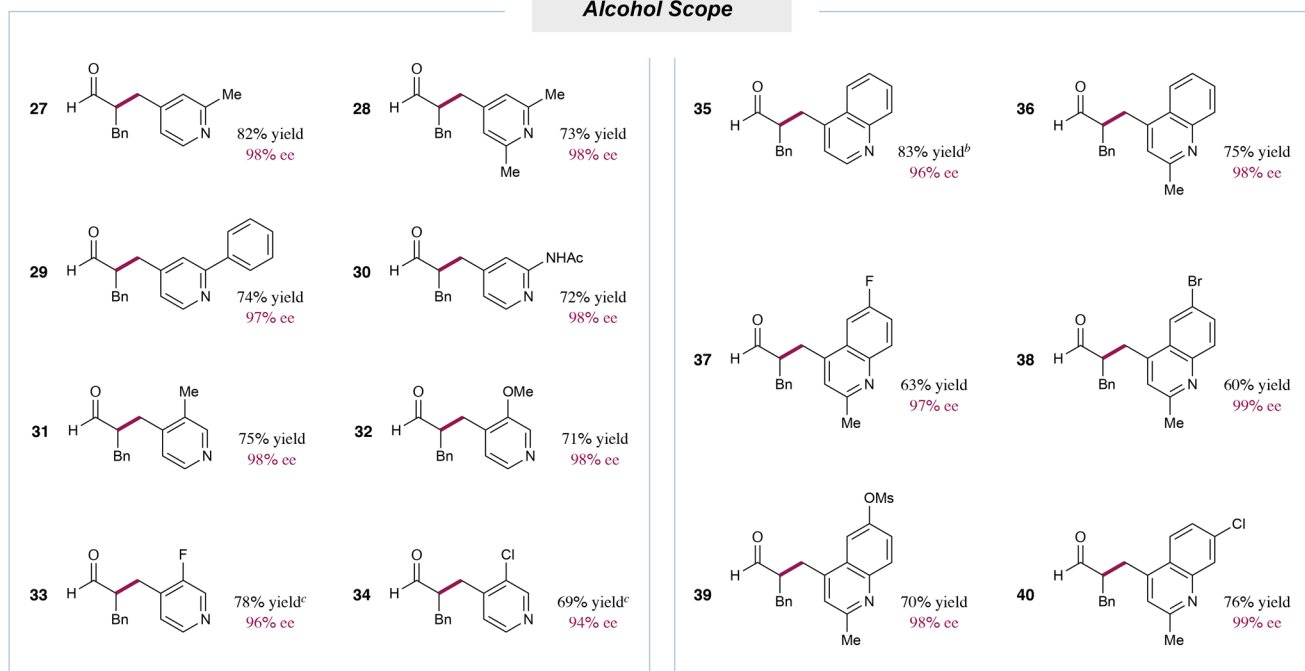
Finally, we sought further to broaden the utility of this spin-center shift paradigm for the enantioselective α -alkylation of aldehydes with unconventional electrophiles as latent alkylating agents. Beyond the heterobenzylic alcohols described above, work by Stephenson and co-workers²³ suggested that alcohols such as α -hydroxy ketones or their derivatives may also be viable electrophiles in this alkylation manifold. While initial experiments demonstrated that free alcohols of this type are not

Table 2. Scope of the Enantioselective α -Benzylation of Aldehydes with Alcohols^a

Aldehyde Scope



Alcohol Scope



^aAlcohol (0.5 mmol), aldehyde (2.0 equiv), lutidine (50 mol %), water (30 equiv), organocatalyst **8** (20 mol %), and photocatalyst **18** (0.5 mol %) were irradiated in DMA with a 34 W blue LED lamp at 0 °C. Isolated yields are reported. Enantioselectivities were determined by chiral HPLC analysis following reduction of the crude aldehydes to the corresponding alcohols. ^bCharacterized as the corresponding alcohol. ^cAldehyde (5.0 equiv). ^dYield determined by ¹H NMR. ^eFrom the Z-starting material, **25** was obtained as a 4.5:1 mixture of Z and E isomers; chiral HPLC analysis was performed following reduction of the crude aldehyde to the corresponding alcohol and subsequent hydrogenation of the alkene.

competent alkylating agents, the corresponding acetates show excellent reactivity (Table 3). Therefore, under slightly modified conditions, octanal (**45**) was alkylated with α -acetoxyacetophenone, as well as the 3,4-(methylenedioxy) and 4-fluoro analogues, to procure the corresponding α -alkyl aldehydes in good yields and high enantioselectivities (**46–48**, 73–80% yield, 87–93% ee).

Notably, these preliminary results demonstrate that an additional class of nontraditional alkylating agents, α -acetoxy ketones, can be activated to this end by a spin-center shift. While acetates are activated leaving groups compared to alcohols (see Table 4 and the associated discussion), they are seldom employed directly in alkylation reactions, as they are still significantly less reactive than typical alkylating agents, such

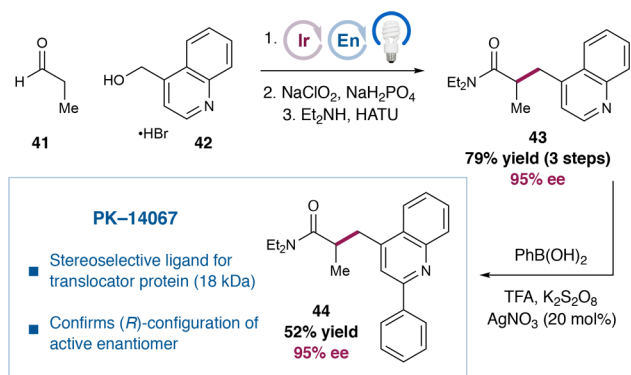
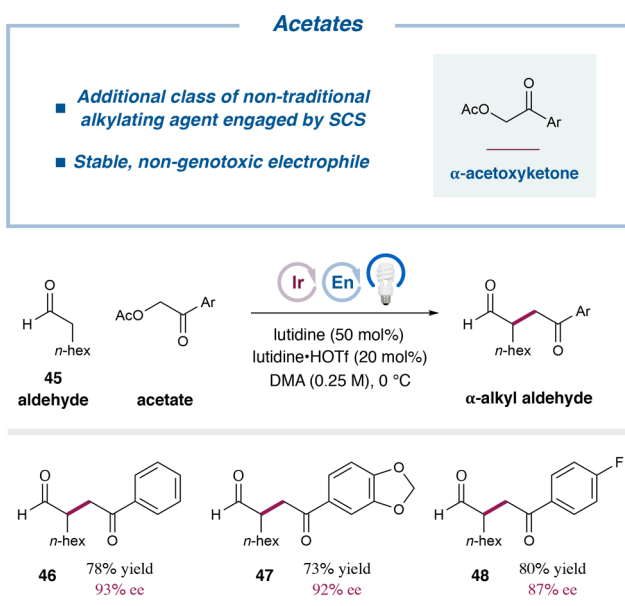


Figure 2. Enantioselective synthesis of stereoselective translocator protein (18 kDa) ligand PK-14067. The enantioselective α -benzylation procedure was conducted using alcohol **42** (2.0 mmol) and aldehyde **41** (5.0 equiv) under conditions listed in Table 2 for 42 h.

Table 3. Spin-Center Shift-Enabled Enantioselective α -Alkylation of Aldehydes with α -Acetoxy Ketones^a



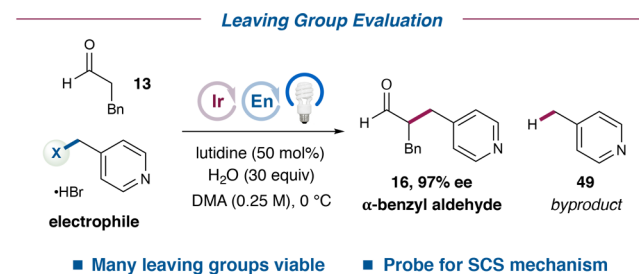
^aAcetate (0.5 mmol), aldehyde **45** (2.0 equiv), lutidine (50 mol %), lutidine·HOTf (20 mol %), organocatalyst **8** (20 mol %), and photocatalyst **18** (0.5 mol %) were irradiated in DMA with a 34 W blue LED lamp at 0 °C. Isolated yields are reported. Enantioselectivities were determined by chiral HPLC analysis.

as alkyl bromides or iodides. Furthermore, like alcohols, they are less genotoxic and more stable than conventional electrophiles.

MECHANISTIC STUDIES

Further investigations were performed to gain a greater mechanistic understanding of the enantioselective α -benzylation of aldehydes with alcohols. Specifically, we sought to determine whether spin-center shift occurs as hypothesized, to elucidate the origin of the major byproduct [i.e., the formation of 4-methylpyridine (**49**) from 4-(hydroxymethyl)pyridine (**3**)] that initially complicated the optimization of this reaction, and to test the possibility of a radical chain mechanism. Thus, three investigations were performed: (1) an examination of how modifications to the leaving group in the electrophile impact reactivity and selectivity, (2) a photocatalyst structure–activity

Table 4. Leaving Group Scope in the Enantioselective Spin-Center Shift-Enabled α -Benzylation of Aldehydes and Its Impact on Reactivity^a



entry	X	E^{red} (V)	K_{SV} (mM ⁻¹)	$\text{p}K_{\text{a}}$ (XH)	yield (2 h)	yield [time]	16:49
1	OAc	-1.19	0.84	4.76	75%	90% [3 h]	18
2	NMe ₃ ⁺ Br ⁻	n.d. ^b	0.13	9.80	67%	86% [5 h]	14
3	OH	-1.29	1.05	15.7	39%	85% [5 h]	7.7
4	OMe	-1.29	1.15	15.2	29%	71% [24 h]	5.1
5	OTBDPS	-1.30	0.82	≈ 13.6	20%	61% [48 h]	3.1
6	-	-1.30	1.30			data for pyridine·HBr	

^aElectrophile (0.25 mmol), aldehyde **13** (2.0 equiv), lutidine (50 mol %), water (30 equiv), organocatalyst **8** (20 mol %), and photocatalyst **18** (0.5 mol %) were irradiated in DMA with a 34 W blue LED lamp. Yields of **16** and **49** were determined by ¹H NMR. Enantioselectivities were determined by chiral HPLC analysis following reduction of the crude aldehyde to the corresponding alcohol. Acidity data in water from ref 24. See the SI for full experimental details. ^bLow solubility prevented electrochemical measurements in aprotic solvents.

relationship (SAR) study, and (3) quantum yield measurements.

To begin, we investigated the impact of the leaving group X on reaction efficiency and chemoselectivity (Table 4). Thus, we prepared a series of (4-pyridyl)methyl electrophiles and subjected them to the standard reaction conditions with hydrocinnamaldehyde (**13**). First, several functional groups aside from alcohols can serve as leaving groups in this transformation. These electrophiles (acetate, trialkylammonium, alkyl ether, and silyl ether) all give rise to α -benzyl aldehyde **16** in respectable to excellent yields (61–90%) and with uniformly high enantioselectivity (97% ee). Further functional groups that do not generally confer alkylating ability can therefore be employed in the outlined enantioselective α -benzylation of aldehydes.

We then sought to account for the different reactivities observed among these electrophiles in order to evaluate our proposal that this reaction proceeds via SCS (Table 4, entries are sorted by decreasing yield and chemoselectivity, the latter parameter being the ratio between yields of desired product **16** and byproduct **49**). Therefore, we measured their reduction potentials (E^{red}) and Stern–Volmer quenching constants (K_{SV}) with photocatalyst **18**, which, in this context, quantifies the relative rates at which the electrophile substrates receive an electron from the excited state of **18**.

Notably, the reduction potentials of the electrophiles (entries 1–5, E^{red} = -1.19 to -1.30 V vs SCE in CH₃CN) are nearly identical both to each other and to that of pyridine·HBr (entry 6, E^{red} = -1.30 V vs SCE in CH₃CN). Such similar potentials suggest that the LUMOs of these compounds all reside primarily on their common structural feature, the protonated heteroaromatic system. If the leaving groups made a significant

contribution to the LUMOs, we would expect a wider range of E^{red} values, given the appreciable stereoelectronic differences between these functionalities. As such, the photoredox activation of these electrophiles likely proceeds via initial SET to the aromatic core, followed by SCS, as proposed in Figure 1 and Scheme 1. For comparison, a conventional electrophile for this reaction, 4-(bromomethyl)pyridine (**50**; see Figure 4),^{14b} is much more easily reduced ($E^{\text{red}} = -0.88$ V vs SCE in CH_3CN for the HBr salt). We propose, therefore, that **50** is engaged by a photoredox catalyst for α -benzylation via direct SET to the C–Br σ^* orbital, rather than by SCS.

The K_{SV} data, in comparison, exhibit appreciable variability among the electrophiles, although no clear relationship is evident between these values and reactivity. Since K_{SV} directly reflects the relative rates of SET between the excited state photocatalyst and the electrophiles, we conclude that this SET is likely rapid, and a subsequent event, such as SCS, dictates reactivity. The measurement of nonzero K_{SV} values also confirms that the excited state photocatalyst is quenched by these electrophiles, consistent with our proposal that the reaction is initiated by SET from the excited photocatalyst to the electrophile.

The observed reactivity trends are best explained by the acid–base properties of the leaving groups. A comparison of the literature $\text{p}K_{\text{a}}$ values for the parent acids (XH) of the leaving groups (X^-) with reaction rates and yields in Table 4 suggests that the electrophiles sort into two classes. First, the more reactive electrophiles possess weakly basic leaving groups (entry 1, X = OAc, and entry 2, X = NMe_3^+). The protonation states of these leaving groups following simple heterolytic C–X scission (anionic carboxylate and neutral trialkylamine, respectively) should be stable in the pyridine/pyridinium reaction buffer. For these electrophiles, therefore, SCS directly follows single-electron reduction of the pyridinium moiety. In contrast, the less reactive electrophiles possess strongly basic leaving groups (entries 3–5, X = OH, OMe, OTBDPS), the corresponding anions of which should be unstable in the reaction medium. These leaving groups must be activated by protonation or hydrogen-bonding before C–X cleavage, and this additional barrier slows the α -benzylation reaction. This clear dependence of reactivity on leaving group acidity suggests that the rate of C–X bond breaking contributes to the overall rate of reaction. A discussion of reactivity trends within the two classes of electrophiles is provided in the SI.

On balance, the data in Table 4 suggest that a rapid SET from the excited state photocatalyst to the electrophile initiates the reaction, followed by slow C–X cleavage (SCS). This step impacts the rate of α -benzylation and is the rate-determining step (RDS) in the linear reaction between the electrophile and the enamine. While these experiments do not assess the kinetics of C–C bond-formation, as they all involve a common electrophilic radical and enamine that would participate in this step, (a) an examination of reactivities among the different alcohol electrophiles employed in Table 2 is consistent with SCS being slower than C–C bond formation, and (b) initial rate studies suggest that the enamine is not involved the RDS of its photoredox-mediated alkylation by the electrophile (see the SI). Higher loadings of either aldehyde or organocatalyst lead to increased rates beyond this initial period, however, as the organocatalytic cycle must turn over to provide further enamine and preliminary experiments suggest that iminium ion hydrolysis is turnover-limiting (also see the SI). The chemoselectivity between desired product **16** and byproduct **49**

(Table 4, final column) is addressed in the following discussion of Figure 3.

Next, we conducted a photocatalyst SAR study. We systematically prepared a series of *tert*-butyl- and methoxy-substituted derivatives of $\text{Ir}(\text{ppy})_3$ and measured their photophysical and electrochemical properties (Figure 3a; also see Figures S3–S35, SI). We then evaluated their performance in the α -benzylation of hydrocinnamaldehyde (**13**) with 4-(hydroxymethyl)pyridine (**3**) and focused on the selectivity between the yields of desired α -benzyl aldehyde **16** and undesired 4-methylpyridine (**49**).

Figure 3a tabulates these results, which are sorted from least selective to most selective (final column). Preliminary examinations of two potentially important properties of these photocatalysts, their excited state lifetimes¹⁷ and Stern–Volmer quenching rates with 4-(hydroxymethyl)pyridine (**3**) (see Figure S53, SI), showed negligible differences. Instead, their electrochemical potentials ($E_{1/2}^{\text{red}}$) seemed to play a primary role in determining selectivity. Since there are four such values to consider (ground-state oxidation by Ir^{IV} , ground-state reduction by Ir^{II} , and excited-state oxidation or reduction by $^*\text{Ir}^{\text{III}}$), we plotted the observed chemoselectivity as a function of each $E_{1/2}^{\text{red}}$ series, as shown in Figure 3b. The strongest correlation ($r^2 = 0.93$) was found between selectivity and $E_{1/2}^{\text{red}}[\text{Ir}^{\text{IV/III}}]$, the oxidizing power of the Ir^{IV} ground state, with lower oxidation potentials leading to higher selectivity. A modest correlation was also found between selectivity and $E_{1/2}^{\text{red}}[\text{Ir}^{*\text{III/II}}]$, the oxidizing ability of the $^*\text{Ir}^{\text{III}}$ excited state ($r^2 = 0.76$). We postulate that this correlation is incidental, however, as the lower oxidation potentials of $^*\text{Ir}^{\text{III}}$ excited states compared to Ir^{IV} ground states suggest that the former species are not responsible for the oxidation leading to **49** (see below). The remaining potentials, $E_{1/2}^{\text{red}}[\text{Ir}^{\text{IV/*III}}]$ and $E_{1/2}^{\text{red}}[\text{Ir}^{\text{III/II}}]$, clearly do not explain the observed trends in chemoselectivity ($r^2 = 0.33$ and 0.24 , respectively).

From the preceding studies, a detailed mechanistic understanding of chemoselectivity emerges, which is outlined in Scheme 2. The electrophile starting material is first reduced by the excited state $^*\text{Ir}^{\text{III}}$ photocatalyst to give radical **51** and an Ir^{IV} species. At this stage, the relative reactivities of radical **51**, enamine **9**, and the Ir^{IV} intermediate dictate the final chemoselectivity. Desired α -benzyl aldehyde **12** is formed (Scheme 2, top) when a spin-center shift occurs to give electrophilic radical **6**, which alkylates enamine **9**. The resulting α -amino radical **10** is oxidized by the Ir^{IV} species to produce iminium ion **11** (see Scheme 1), which is hydrolyzed to deliver **12**. Major byproduct **49** arises (Scheme 2, bottom) when the Ir^{IV} species oxidizes enamine **9** directly. This SET presumably leads to radical **52**, which formally reduces electrophilic radical **6**, likely with the assistance of the photocatalyst. The resulting byproducts are thus the previously discussed **49**, from net alcohol reduction, and oxidized organocatalyst **53**,²⁵ which we have also isolated from several reaction mixtures.²⁶

This description accounts for the chemoselectivity trends outlined in Table 4 and Figure 3 in terms of two competing pathways for the Ir^{IV} intermediate. Desired α -benzyl aldehyde **12** is obtained when the Ir^{IV} species oxidizes the strongly reducing α -amino radical **10** ($E_{1/2}^{\text{ox}} = -0.92$ to -1.12 V vs SCE in CH_3CN for simple α -amino radicals),¹⁸ an SET which should be rapid and irreversible for all photocatalysts employed in this investigation ($E_{1/2}^{\text{red}}[\text{Ir}^{\text{IV/III}}] = +0.34$ V to $+0.70$ V vs SCE in CH_2Cl_2 ; see Figure 3). Conversely, undesired

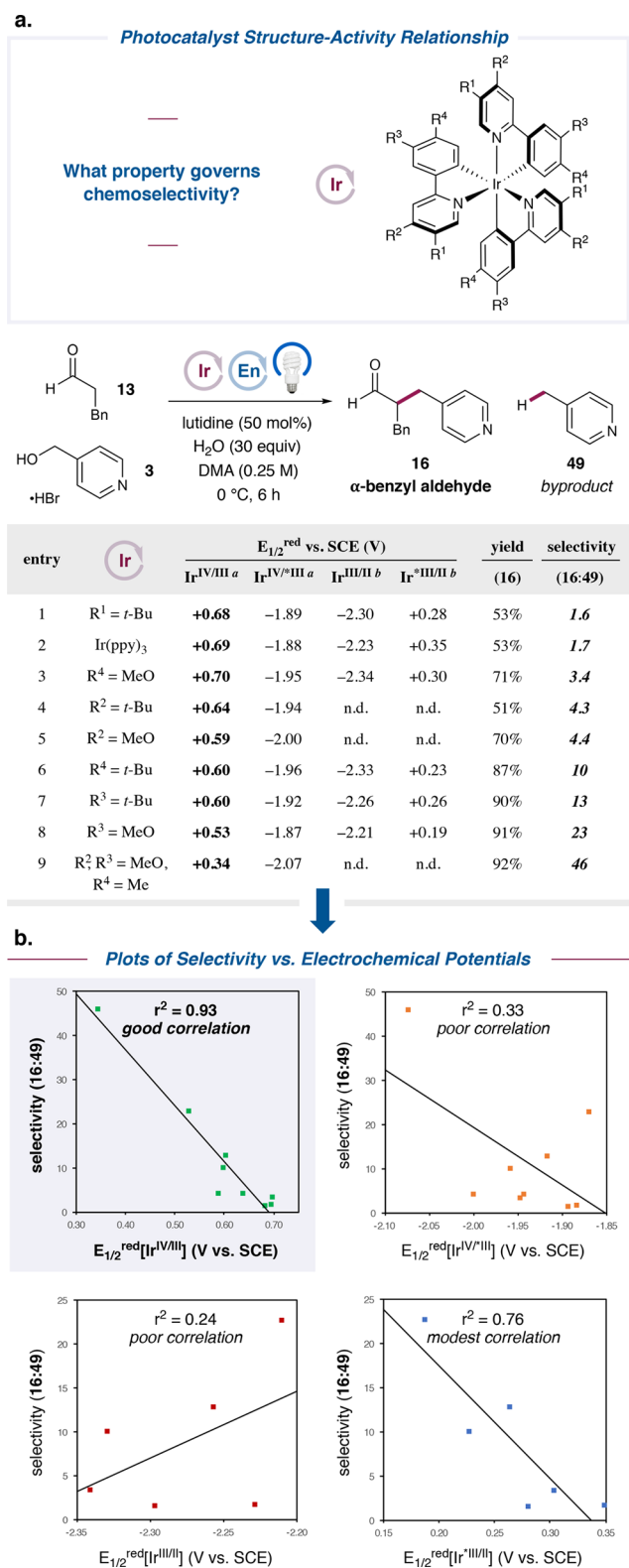


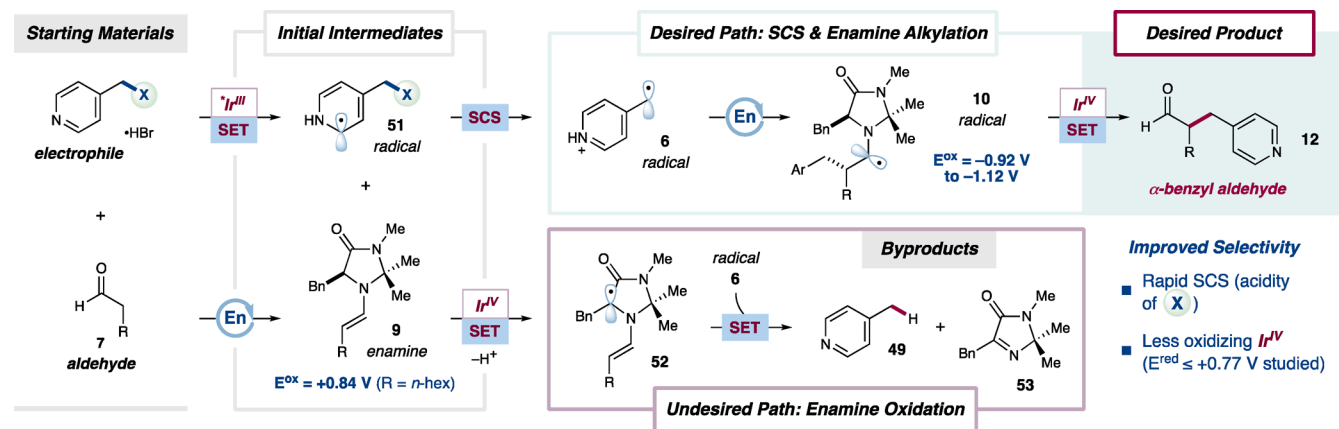
Figure 3. Impact of photocatalyst structure on chemoselectivity in the α -benzylation of aldehydes with alcohols. (a) Alcohol 3 (0.25 mmol), aldehyde 13 (2.0 equiv), lutidine (50 mol %), water (30 equiv), organocatalyst (\pm)-8 (20 mol %), and photocatalyst (0.5 mol %) were irradiated in DMA with a 34 W blue LED lamp. Yields of 16 and 49 were determined by ^1H NMR. (b) Plots of selectivity vs each electrochemical potential. ^aMeasured in CH_3CN . ^bMeasured in CH_2Cl_2 .

byproducts 49 and 53 form when the Ir^{IV} species oxidizes enamine 9 ($E^{\text{ox}} = +0.84$ vs SCE in CH_3CN for $\text{R} = n\text{-hex}$). This SET is feasible, albeit endergonic, for all the above-listed Ir^{IV} oxidation potentials (see above for data in CH_2Cl_2 ; for photocatalysts soluble in CH_3CN , $E_{1/2}^{\text{red}}[\text{Ir}^{\text{IV/III}}] \leq +0.77$ V vs SCE in this solvent; see the SI). Furthermore, appreciable concentrations of enamine 9 are present throughout the reaction, whereas radical 10, which must be oxidized to obtain the desired product, should only be present in trace amounts.

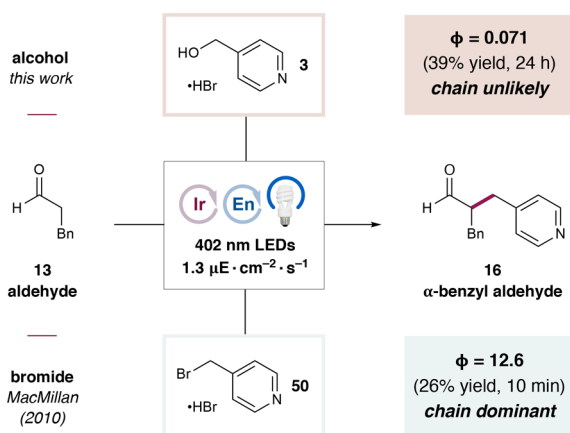
With respect to the electrophile, the least basic leaving groups give the highest chemoselectivities (see Table 4) due to the corresponding acceleration of the SCS step. While SCS must occur to form both desired α -benzyl aldehyde 12 and byproduct 49, the rate of this elementary step has a different impact on the pathways leading to each product. In the limiting case when SCS is fast, α -amino radical 10 forms rapidly, and this strong reductant reacts preferentially with the Ir^{IV} intermediate to close the photocatalytic cycle and generate desired product 12. Conversely, when SCS is slow, 10 is unavailable to reduce the Ir^{IV} species. Instead, enamine 9 can be oxidized by the Ir^{IV} intermediate, giving 52 (or a related species) after proton transfer. Radicals such as 52 should be modest reducing agents, and upon the eventual formation of electrophilic radical 6, its formal reduction by 52 (likely mediated by a photocatalyst) competes with C–C bond formation, ultimately producing 49 and 53.

With respect to the photocatalyst, selectivity for desired product 12 increases straightforwardly with decreasing Ir^{IV} oxidation potentials. Lower Ir^{IV} potentials render undesired enamine oxidation increasingly endergonic, while oxidation of the strongly reducing radical 10 remains highly exergonic and ensures that the desired product can still be accessed without complication. Indeed, as shown in Figure 3, chemoselectivity rises from modest levels when using photocatalysts with the most oxidizing Ir^{IV} states (entries 1–3, 16:49 = 1.6:1 to 3.4:1 for $E_{1/2}^{\text{red}}[\text{Ir}^{\text{IV/III}}] = +0.68$ to $+0.70$ V vs SCE in CH_2Cl_2) to excellent when using the least oxidizing derivative, which we designed explicitly for this purpose (entry 9, 16:49 = 46:1 for $E_{1/2}^{\text{red}}[\text{Ir}^{\text{IV/III}}] = +0.34$ V vs SCE in CH_2Cl_2).

Finally, we questioned whether a radical chain propagation mechanism could be occurring in this transformation, as work by Yoon et al. has demonstrated that such pathways operate in a range of photoredox-catalyzed transformations,²⁷ including the enantioselective α -alkylation of aldehydes with alkyl bromides.^{14a} With the present alcohol electrophiles, however, we hypothesized that the relatively difficult reduction of the model substrate (3, $E^{\text{red}} = -1.29$ V vs SCE in CH_3CN for the HBr salt) would prohibit its reduction by any organic intermediates formed during the reaction (the most likely candidate would be α -amino radical 10, depicted in Schemes 1 and 2, but the literature data suggest that the potentials of simple analogues, $E_{1/2}^{\text{ox}} = -0.92$ to -1.12 V vs SCE in CH_3CN , are still insufficiently reducing).¹⁸ As shown in Figure 4, the quantum yield for the reaction of alcohol 3 with hydrocinnamaldehyde (13) is 0.071. While this observation does not rule out propagation events conclusively, the relatively low value is consistent with our mechanistic hypothesis that each photon absorbed by the photocatalyst should lead, at most, to a single product molecule. In contrast, we surmised that the formation of reducing intermediates such as 10 would enable radical chain propagation events when a more easily reduced electrophile, such as the corresponding benzylic bromide (50), is employed ($E^{\text{red}} = -0.88$ V vs SCE in CH_3CN for the HBr

Scheme 2. Mechanistic Description of Chemoselectivity in the Enantioselective SCS-Enabled α -Benzylation of Aldehydes

Quantum Yield Measurement

Figure 4. Quantum yield determination for the enantioselective α -benzylation of aldehydes with alcohols and bromides.

salt). Indeed, for the α -benzylation of hydrocinnamaldehyde (**13**) with **50**, under the optimal conditions for benzylic bromide electrophiles reported in 2010, we measured a quantum yield of 12.6. In this reaction, therefore, the photocatalyst serves primarily as an initiator for a self-propagating chain responsible for the majority of product formation.

CONCLUSIONS

We have developed a strategy based on spin-center shift that enables the enantioselective α -benzylation of aldehydes with electron-deficient heterobenzylic alcohols. To our knowledge, this work represents the first example of a direct enantioselective α -alkylation of carbonyl compounds with alcohols where the electrophile does not contain specialized cation-stabilizing features to promote $\text{S}_{\text{N}}1$ -type activation. Additional nontraditional leaving groups, such as acetates and ethers, are also competent in this reaction, and α -acetoxy ketone electrophiles can be employed to access a further aldehyde α -alkylation motif via SCS. Mechanistic studies are consistent with spin-center shift as a key elementary step and elucidate the impact of electrophile and photocatalyst structures on reactivity. Finally, enamine oxidation was identified as the origin of the major side

reaction, enabling optimal yields to be obtained by rational photocatalyst design.

ASSOCIATED CONTENT

Supporting Information

The Supporting Information is available free of charge on the ACS Publications website at DOI: 10.1021/jacs.7b12768.

Experimental procedures and compound characterization data (PDF)

AUTHOR INFORMATION

Corresponding Author

*dmacmill@princeton.edu

ORCID

David W. C. MacMillan: 0000-0001-6447-0587

Notes

The authors declare no competing financial interest.

ACKNOWLEDGMENTS

Financial support was provided by the NIHGMS (R01 GM-103558-05) and kind gifts were from Merck, Abbvie, BMS, and Janssen. E.D.N. acknowledges the NIH for a postdoctoral fellowship (F32 GM119362-01A1).

REFERENCES

- (1) Eklund, H.; Uhlin, U.; Färnegårdh, M.; Logan, D. T.; Nordlund, P. *Prog. Biophys. Mol. Biol.* **2001**, *77*, 177.
- (2) Wessig, P.; Muehling, O. *Eur. J. Org. Chem.* **2007**, *2007*, 2219.
- (3) Dryzhakov, M.; Richmond, E.; Moran, J. *Synthesis* **2016**, *48*, 935.
- (4) Henkel, T.; Brunne, R. M.; Müller, H.; Reichel, F. *Angew. Chem., Int. Ed.* **1999**, *38*, 643.
- (5) Jin, J.; MacMillan, D. W. C. *Nature* **2015**, *525*, 87.
- (6) (a) Narayanam, J. M. R.; Stephenson, C. R. J. *Chem. Soc. Rev.* **2011**, *40*, 102. (b) Xuan, J.; Xiao, W. J. *Angew. Chem., Int. Ed.* **2012**, *51*, 6828. (c) Prier, C. K.; Rankic, D. A.; MacMillan, D. W. C. *Chem. Rev.* **2013**, *113*, 5322. (d) Schultz, D. M.; Yoon, T. P. *Science* **2014**, *343*, 1239176. (e) Skubi, K. L.; Blum, T. R.; Yoon, T. P. *Chem. Rev.* **2016**, *116*, 10035. (f) Shaw, M. H.; Twilton, J.; MacMillan, D. W. C. *J. Org. Chem.* **2016**, *81*, 6898.
- (7) Evans, D. A.; Ennis, M. D.; Mathre, D. J. *J. Am. Chem. Soc.* **1982**, *104*, 1737.
- (8) Oppolzer, W.; Moretti, R.; Thomi, S. *Tetrahedron Lett.* **1989**, *30*, 5603.
- (9) Seebach, D.; Wasmuth, D. *Helv. Chim. Acta* **1980**, *63*, 197.
- (10) Myers, A. G.; Yang, B. H.; Chen, H.; Gleason, J. L. *J. Am. Chem. Soc.* **1994**, *116*, 9361.

- (11) Maruoka, K.; Ooi, T. *Chem. Rev.* **2003**, *103*, 3013.
- (12) Imai, M.; Hagihara, A.; Kawasaki, H.; Manabe, K.; Koga, K. *J. Am. Chem. Soc.* **1994**, *116*, 8829.
- (13) Doyle, A. G.; Jacobsen, E. N. *J. Am. Chem. Soc.* **2005**, *127*, 62.
- (14) (a) Nicewicz, D. A.; MacMillan, D. W. C. *Science* **2008**, *322*, 77. (b) Shih, H.-W.; Vander Wal, M. N.; Grange, R. L.; MacMillan, D. W. C. *J. Am. Chem. Soc.* **2010**, *132*, 13600. (c) Zhu, Y.; Zhang, L.; Luo, S. *J. Am. Chem. Soc.* **2014**, *136*, 14642. (d) Welin, E. R.; Warkentin, A. A.; Conrad, J. C.; MacMillan, D. W. C. *Angew. Chem., Int. Ed.* **2015**, *54*, 9668.
- (15) Bohlmann, R. Synthesis of Halides. In *Comprehensive Organic Synthesis*; Trost, B. M., Ed.; Pergamon: Oxford, 1991; Vol. 6, pp 203–220.
- (16) (a) Cozzi, P. G.; Benfatti, F.; Zoli, L. *Angew. Chem., Int. Ed.* **2009**, *48*, 1313. (b) Guo, Q.-X.; Peng, Y.-G.; Zhang, J.-W.; Song, L.; Feng, Z.; Gong, L.-Z. *Org. Lett.* **2009**, *11*, 4620. (c) Capdevila, M. G.; Benfatti, F.; Zoli, L.; Stenta, M.; Cozzi, P. G. *Chem. - Eur. J.* **2010**, *16*, 11237. (d) Ikeda, M.; Miyake, Y.; Nishibayashi, Y. *Angew. Chem., Int. Ed.* **2010**, *49*, 7289. (e) Song, L.; Guo, Q.-X.; Li, X.-C.; Tian, J.; Peng, Y.-G. *Angew. Chem., Int. Ed.* **2012**, *51*, 1899. (f) Mo, X.; Hall, D. G. *J. Am. Chem. Soc.* **2016**, *138*, 10762.
- (17) Dedeian, K.; Djurovich, P. I.; Garces, F. O.; Carlson, G.; Watts, R. J. *Inorg. Chem.* **1991**, *30*, 1685.
- (18) Wayner, D. D. M.; Dannenberg, J. J.; Griller, D. *Chem. Phys. Lett.* **1986**, *131*, 189.
- (19) Zuo, Z.; MacMillan, D. W. C. *J. Am. Chem. Soc.* **2014**, *136*, 5257.
- (20) Dubroeuq, M.-C.; Bénavidès, J.; Doble, A.; Guilloux, F.; Allam, D.; Vaucher, N.; Bertrand, P.; Guérémy, C.; Renault, C.; Uzan, A.; Le Fur, G. *Eur. J. Pharmacol.* **1986**, *128*, 269.
- (21) Seiple, I. B.; Su, S.; Rodriguez, R. A.; Gianatassio, R.; Fujiwara, Y.; Sobel, A. L.; Baran, P. S. *J. Am. Chem. Soc.* **2010**, *132*, 13194.
- (22) Brouwer, C.; Jenko, K.; Zoghbi, S. S.; Innis, R. B.; Pike, V. W. J. *Med. Chem.* **2014**, *57*, 6240.
- (23) Nguyen, J. D.; Matsuura, B. S.; Stephenson, C. R. J. *J. Am. Chem. Soc.* **2014**, *136*, 1218.
- (24) (a) Bacarella, A. L.; Grunwald, E.; Marshall, H. P.; Purlee, E. L. *J. Org. Chem.* **1955**, *20*, 747. (b) Berg, U.; Jencks, W. P. *J. Am. Chem. Soc.* **1991**, *113*, 6997. (c) Reeve, W.; Erikson, C. M.; Aluotto, P. F. *Can. J. Chem.* **1979**, *57*, 2747. (d) Arm, H.; Hochstrasser, K.; Schindler, P.-W. *Chimia* **1974**, *28*, 237.
- (25) Walaszek, D. J.; Rybicka-Jasińska, K.; Smoleń, S.; Karczewski, M.; Gryko, D. *Adv. Synth. Catal.* **2015**, *357*, 2061.
- (26) Imine **53** is the only oxidative byproduct we have isolated, though it does not account fully for the generation of **49**. A small amount of nonspecific aldehyde decomposition also occurs that could account for the formation of **49**, and we can detect trace quantities of cinnamaldehyde in situ in reactions employing aldehyde **13**, but the full array of byproducts resulting from **52** has yet to be elucidated. H atom abstraction from solvent by **6** does not occur, as no D-incorporation into **49** is observed when conducting the reaction in DMF-*d*₇.
- (27) Cismesia, M. A.; Yoon, T. P. *Chem. Sci.* **2015**, *6*, 5426.

■ NOTE ADDED AFTER ASAP PUBLICATION

The toc/abstract graphic was corrected February 23, 2018.